Colloids and Surfaces B: Biointerfaces 178 (2019) 385–394

Contents lists available at ScienceDirect

Colloids and Surfaces B: Biointerfaces

journal homepage: www.elsevier.com/locate/colsurfb

Nanostructured titanium oxide hybrids-based electrochemical biosensors for healthcare applications

Nagaraj P. Shetti[a,*], Shikandar D. Bukkitgar[a], Kakarla Raghava Reddy[b,*], Ch. Venkata Reddy[c,*], Tejraj M. Aminabhavi[d]

[a] Electrochemistry and Materials Group, Department of Chemistry, K. L. E. Institute of Technology, Gokul, Hubballi 580030, India[1]
[b] School of Chemical and Biomolecular Engineering, The University of Sydney, Sydney, NSW 2006, Australia
[c] School of Mechanical Engineering, Yeungnam University, Gyengsan 712-749, South Korea
[d] Sonia College of Pharmacy, Dharwad, 580 002, Karnataka, India

ARTICLE INFO

Keywords:
Nanostructures
Metal oxides
Nanohybrids
Electrochemistry
Hybrid electrodes
Electrochemical sensors

ABSTRACT

Biosensors are promising biotechnology products that can be widely used for environmental monitoring, food analysis, and healthcare diagnostics. To detect analytes of interest, the use of nanotechnology in bio-analytical devices is advantageous for increased sensitivity, device simplification, and rapid sensing with multiple capabilities. Depending on the application, biosensors can be fabricated from different materials. TiO_2 is a semiconductor material and has received significant attention for various applications such as sensors, solar cells, water splitting, etc. The wide applicability of recently developed novel composition and structure of TiO_2 materials has accelerated the development and miniaturization of biosensor devices. This study focuses on recent achievements in TiO_2 nanostructured hybrids-based biosensors for detecting various biological markers important for healthcare.

1. Introduction

In the fields of healthcare, biological analysis, food safety, environmental monitoring, and chemical analysis, biosensors have become an important practical tool. When compared to conventional analytical methods, biosensors are much smaller devices which provide real-time information and are ideal for rapid measurement and analysis. The increasing demand for simple, cost-effective, rapid, and portable screening methods in medical research, agricultural inspection, industrial quality control, and food safety has accelerated the development of biosensors. The improvement of biosensors requires interdisciplinary collaboration involving physics, materials science, chemistry, and life sciences. Enzyme-based sensors require complicated enzyme immobilization and exhibit a limited lifetime due to deactivation of the immobilized enzyme. Furthermore, the properties of the bioactive layer associated with transducers govern biosensor performance. Therefore, retaining high electroactivity of the protein or enzyme on the electrode surface is crucial. Research interest in nanostructured materials has considerably increased in recent years due to their high active surface area and regular size.

Monitoring of various molecules present in biological systems and the environment has garnered significant interest in the field of nanotechnology [1,2]. The novel and multifunctional properties of nanoparticles have attracted a diverse research community with interests in various fields such as food, security, transportation, and health. The smart and efficient usage of nanomaterials has the potential to enhance electronic device performance while improving detection limits and sensitivity. However, the availability of commercialized biosensors is currently lacking, but rigorous efforts have been made to improve the accuracy, miniaturization, analysis speed, and resolution of biosensor-based devices. Applications involving nanomaterials in the medical field include drug delivery, point-of-care diagnostics, imaging, and biomaterials. The unique properties of nanostructured metal nanoparticles such as gold, silver, and nickel, as well as semiconductor materials including ZnO, TiO_2, CeO_2, and SnO_2 have found many applications in the development of biosensors.

Since the discovery of photocatalytic water splitting using ultraviolet light on the surface of TiO_2 by Fujishima and Honda [3–5] in 1972, increasing interest in the field has led to many developments. Application of TiO_2 nanoparticles is widespread in a variety of promising fields such as photocatalysis, photovoltaics, and sensors [6–9]. In addition, TiO_2 nanoparticles are photo-corrosion resistant,

* Corresponding authors.
E-mail addresses: dr.npshetti@gmail.com (N.P. Shetti), reddy.chem@gmail.com (K.R. Reddy), cvrphy@gmail.com (C.V. Reddy).
[1] Affiliated to Visvesvaraya Technological University, Karnataka.

https://doi.org/10.1016/j.colsurfb.2019.03.013
Received 11 December 2018; Received in revised form 20 February 2019; Accepted 6 March 2019
Available online 16 March 2019
0927-7765/

biocompatible, nontoxic, and can be produced on a large-scale under mild conditions leading to low-cost fabrication and widespread utilization of these particles [10–13]. Recently, the use of TiO_2 nanomaterials with improved composition and structure in the form of sensing devices has been developed [14–17]. The sensors can be classified based on their sensing targets or working principle, with groups including electric [14], gas [18,19], humidity [20], environmental [21], optical [22], and biosensors [23].

Hence, a review about the sensors-based healthcare applications should be carried out. In the current review, we report the recent achievements in TiO_2 nanostructured hybrids-based sensors. Fabrication strategies, control of morphological structures, influencing parameters for enhancing sensing characteristics of TiO_2-based nanohybrids for detecting various biological markers are discussed in detail. Furthermore, we also described future perspectives on using these materials for sensing applications.

1.1. Phases of TiO_2

Anatase, brookite, and rutile are the three natural TiO_2 phase structures with band gaps of 3.2, 3.02, and 2.96 eV, respectively [24,25]. The increased stability of anatase and rutile compared to that of brookite facilitates their wider application. In rutile and anatase TiO_2, a single unit cell consists of 6 atoms (Fig. 1) and the TiO_6 octahedron is relatively more distorted in anatase compared to that of rutile [26–28]. TiO_2 materials are environmentally friendly and biocompatible with ideal properties for a potential interface to immobilize biomolecules [29,30]. The bio catalytic activity of enzymes immobilized on TiO_2 materials is maintained by coordination bond formation with amine and carboxyl groups in the enzymes [31,32]. The biosensing ability of the TiO_2 material is typically related to structural properties, valance band location, and hole generation and availability at the surface of the material to be harvested by outer free electrons. The reaction between the analyte and biomolecule produces electrons which are easily collected by TiO_2 due to its electron accepting character.

A variety of samples including cell cultures, bodily fluids, and food can be analyzed using biosensors [33]. High selectivity and sensitivity can be achieved in biosensors via specific binding affinity of the immobilized biological recognition elements to the target compounds. Due to the previously mentioned merits of TiO_2 nanomaterials, they hold great promise for the immobilization of biological components [34,35].

1.2. Methods for synthesis of hybrid nanoparticles

TiO_2 nanoparticles can be synthesized using different methods including electro-deposition [36–38], hydrothermal [39–42], sol–gel [43–45], chemical vapor deposition (CVD) [46–48], physical vapor deposition [49–51], micelle/inverse micelle, and direct oxidation techniques. The TiO_2 crystal structure synthesized can be controlled to favor anatase, rutile or amorphous phases using the above-mentioned methods. The precise phase structures can be created by adjusting the temperature and pressure to certain values. Furthermore, TiO_2 nanomaterial geometry can be altered to achieve nanosphere, one-dimensional, and three-dimensional nanostructures. Recently, researchers have developed TiO_2 nanomaterials with different structures. However, the present investigations have focused on the synthesis of TiO_2 nanomaterials with prime importance on usage of dopant and development of composite material to improve the properties of TiO_2 nanomaterials.

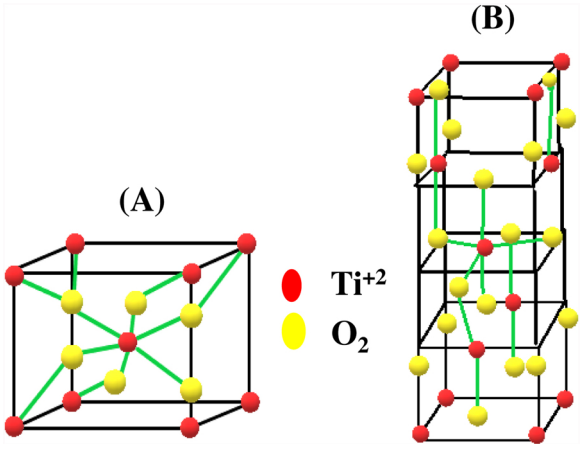

Fig. 1. Structure of TiO_2. (A) Rutile, (B) anatase.

Development of innovative strategies to prepare nanomaterials consisting of desired properties have attracted researchers in the field of material science. To control the extrinsic properties and to obtain materials with define architecture, and desired properties for targeted applications, agglomeration of nanoparticles appears to be an ideal approach. To control the intrinsic properties, doping nanomaterials with metal ions is a promising and effective way.

Generally, the synthesis of nanoparticles could be categorized into two domains: physical and chemical methods. The physical methods are simpler as compared to chemical methods but the control of size of hybrid nanoparticles are complex. Whereas, the chemical method of synthesis of hybrid nanoparticles provide a better performance along with controlled nanostructures and a strong hybridization between nanoparticles is obtained. Further, the chemical method for synthesis of hybrid nanoparticles exhibits unsolicited properties due to the presence of chemical species such as polymer shells, stabilizing agents. In addition, within the final nanostructures, the individual nanoparticles remain sometimes separate and distinct.

Hybrid nanoparticles can be synthesis either by the reduction of metal precursor or by the processing routes. The reduction of metal precursors, chemical reduction and photoreduction methods can be used. Further, hybrid nanoparticles can be fabricated by various processing routes such as thermal decomposition, hydrothermal, coprecipitation, sol–gel, sonochemical, electrodeposition, and seeding growth.

1.2.1. Chemical reduction (CR) and photoreduction (PR) methods

These methods are usually performed to obtain deposition of noble metals nanoparticles on the surface of oxide metal nanoparticles to form noble metal decorated oxide metal nanoparticles. The synthesis process involves adsorption of noble metal ions on the surface of oxide metal nanoparticles and then chemical reducing agents or by photoirradiation (in PR method) are used for the reduction reaction, assisted with ultrasonication sometimes for the synthesis. However, the drawback such as, the mixture of both pure noble metal nanoparticles and hybrid nanoparticles can be resolved by (i) by using local immobilization of chemical reducing agent on the surface of OM nanoparticles [52]; (ii) by using a redox reaction of metal hydroxide and noble metal ion (without using the reducer [53]); and (iii) by using a low weight ratio of NM precursors and OMs (e.g., NMs:OMs, 1:30).

Considering the photoreduction method, photoelectrons form oxide metals play a crucial role during the process upon radiation of light. The free electrons from transition metal act with metal ions on the surface to form nanoparticles on the hosting nanoparticles surface (Figs. 2 and 3).

1.2.2. Sol–gel method

Sol–gel method is one of the most common methods used for the synthesis of hybrid nanoparticles. Various hybrid nanostructures can be obtained depending upon the ligand/surfactant/stabilizers used during the synthesis. The size of the hybrid nanoparticles are accurately controllable, however, the bonding/hybridization between hybrid nanoparticles is relatively weak.

Giampiccolo et al. synthesized TiO_2 and graphene/TiO_2 hybrids through a simple sol–gel method as a multifunctional material, for catalytic and gas sensing activity, for monitoring NO_2 with the aid of

Fig. 2. Synthesis step for hybrid nanoparticles by chemical reduction method.

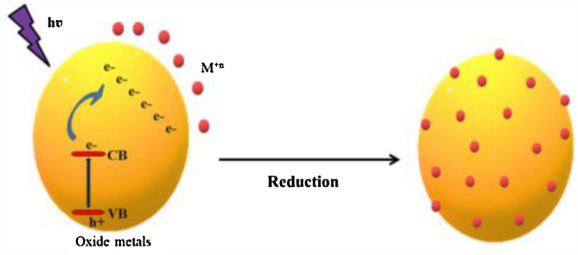

Fig. 3. Synthesis step for hybrid nanoparticles by the chemical reduction method.

UV- or Vis-light. The graphene/TiO_2 hybrids were synthesized by two methods, one involved the addition of graphene to the reaction vessel prior to initiating the sol–gel reaction followed by annealing ($GTiO_2S$) and the other was an addition of graphene to TiO_2 nanoparticles which had already been annealed ($GTiO_2M$). It was further suggested that the conductometric sensor based on $GTiO_2S$ was having higher response to NO_2 as compared to that of TiO_2 and $GTiO_2M$ [54].

Talane et al. [55] proposed a sol–gel method for the preparation of pure and erbrium-doped TiO_2 with anatase structure. The synthesized nanoparticles were poly-crystalline in nature and the size decreased with increasing concentration of Er^{+3} ions, implying that the growth of crystallite is hindered due to the presence of dopant ions on the grain boundary. With the increasing concentration of erbium the crystalline nature reduced due to the substitution of Er^{+3} ions into the site of Ti^{+4} leading to disorder. The findings were important in terms to understand the optical, structural and luminescence properties of erbrium doped TiO_2 nanoparticles for use in a bio-imaging device, light emitting devices and solar cells. The proposed methodology for the synthesis of erbium-doped TiO_2 luminescent nanoparticles with uniform shape, size and crystalline phase is essential to control their properties and exploring their potential application in various fields.

Wei et al. [56] synthesized Sn-doped TiO_2 nanoparticles by sol–gel method assisted by ultrasonic assistance. Synthesizing anatase crystalline TiO_2 nanoparticles with the high specific surface area are significantly important in promoting photo-catalytic activity and in industrial application. However, it has been observed that the amorphous TiO_2 aerogels have to be calcined at high temperature to improve the crystalline property of TiO_2 aerogels. This leads to a decrease in the specific surface area due to the collapse of the aerogel framework. Hence, direct synthesizing of crystalline phase without annealing and in the ultrasonic-assisted sol–gel process is significant. The results confirmed the Sn-doped TiO_2 aerogels had a co-existing phase with high specific area and micropores which could be converted into mesopores.

TiO_2 with tetragonal anatase phase consisting of an average crystalline size of 10–14 nm was synthesized by sol–gel method. Further the addition of neodymium as dopant suggested the presence of separate peak in XRD pattern at $2\theta = 31.78$ (1 2 1) indicated the presence of brookite phase of TiO_2 and the presence of the rutile phase was confirmed from peaks at $2\theta = 45.48$ (2 1 0) and 55.10 (1 1 0). 100% anatase phase was observed for pure TiO_2 nanoparticles were as the Nd-doped TiO_2 nanoparticles consisted of a mixture of anatase, rutile and brookite phases of TiO_2 nanoparticles. Increasing the concentration of Nd dopant decreased the mass fraction of anatase phase. The phase transformation was significantly affected by the acid concentration and temperature. The growth of TiO_2 nanoparticles was inhibited due to adsorption of Nd ions, hence the crystallite size decreased with increasing concentration of Nd. The FESEM investigations suggested the spherical-like particles with irregular arrangement and non-uniform distribution [57].

1.2.3. Hydrothermal and thermal decomposition processes

These methods are advantages in ease controlling of the size and shape of nanoparticles. High temperature and pressure are usually required by the hydrothermal process, whereas multiple steps are involved in thermal decomposition.

Mehraz et al. [58] proposed a method for large scale production of Sn-doped TiO_2 nanoparticles using the hydrothermal method. Size and the shape of prepared nanoparticles were strongly dependent on the temperature and the Sn doping content. TiO_2 phase and morphology transformation were promoted by dopant depending on the synthesizing temperature. The increasing amount of added Sn dopant increased the size of TiO_2 nanoparticle building units from 9.8 to 30.4 nm and reduced its band gap energy at certain Sn dopant amount threshold. At a temperature below 100 °C, increasing Sn doping produced rutile phase, whereas above 100 °C the main phase was anatase and not affected by Sn dopant content. At higher temperature shape change from less spherical to hexagonal plate shape was induced by Sn doping. Concluding that Sn doping amount has a significant influence on the optical and structural properties of Sn-doped TiO_2.

Viet et al. [59] reported a one-step hydrothermal process for the synthesis of Si-doped TiO_2 nanotubes from commercially available SiO_2 and TiO_2. The morphological investigations suggested that the Si atoms were well embedded into the crystal lattices of TiO_2 nanotubes. The synthesized nanotubes were uniform and the diameter of the nanotube was of 8 ± 2 nm with a length of 100–200 nm. The XRD analysis of Si-doped TiO_2 nanotubes suggest the appearance of three peaks at $2\theta = 24^\circ$, 48°, and 61° corresponding to (101), (200), and (204) crystal lattice planes of anatase phase of TiO_2 and at $2\theta = 27.25^\circ$ corresponds to (110) plane of rutile phase of TiO_2.

Sun et al. [60] proposed a method for immobilization of TiO_2 nanotubes on carbon fibers based on alkali treatment of TiO_2 nanowires using hydrothermal process. The results obtained from the characterization of these nanomaterials suggested that the entire surface of carbon fibers were covered with TiO_2 nanotubes having the inner and outer diameter of ca 4.6 and 8.7 nm, respectively. The EDS (energy dispersive spectrometer) and XPS (X-ray photoelectron spectrometer) analysis suggested that the main elements present on the surface of carbon fibers/TiO_2 nanotubes were C, O, and Ti. XRD analysis revealed the transformation of titanate nanotubes to anatase TiO_2 nanotubes. The key finding suggested that a flexible non-metallic substrate can be used efficiently for the immobilization of TiO_2 nanotubes.

1.2.4. Coprecipitation method

This method is simple and efficient, but after the formation of nanoparticles, they undergo formation of clusters and these clusters join to form aggregates and hen further agglomerates very quickly. In addition, sedimentation of the whole precipitate occurs depending upon the properties and the density of the nanoparticles. To prevent this, in situ stabilizers are used to keep the particles in nano form which cover their surface immediately after the formation of nanoparticles.

Ma et al. [61] proposed a possible growth mechanism of Ag–Fe_3O_4 core–shell nanowires by coprecipitation method. In aqueous solution, silver nanowires were used as the nucleation site for the growth of Fe_3O_4. Simple adjustments in reaction conditions such as the concentration of $FeCl_3/FeCl_2$, poly (vinylpyrrolidone), reaction

temperature, and time allowed easy control of size and morphology of core-shell nanowires.

In addition, recent years have witnessed significant importance for the synthesis of composite material [62–65]. Development of photo-catalyst that have activity under visible irradiation and low re-combination of photo-generated electron/hole pair is significant in the application of TiO_2 nanomaterials in wide applications. The research has been explored and investigated various compounds in this contest. Rodríguez et al. [66] synthesized bismuth oxychloride (BiOCl) TiO_2 composite by sol–gel method. BiOCl is a tetragonal structure consisting of Cl-Bi-O-Bi-Cl sheets, developing an electric field which is generated by an inner layer of $\{Bi_2O_2\}^+$ interacting with Cl- ions by Van der Waals force and induce higher separation of electron/hole pair.

Bismuth vanadate ($BiVO_4$) has been widely investigated for its excellent performance in ferroelastic and paraelastic, acoustic-optical properties, photocatalysts, and ionic conductivity. Oliveira et al. [67] reported the dielectric and structural characterization of composite synthesized from the mixture of BiVO4and TiO_2. The investigations suggested that the addition of TiO_2 improves the thermal stability of the composites.

There are reports suggesting the synthesis of various TiO_2 composite material such as polydopamine/TiO_2 [68], wollastonite@TiO_2 [69], NiO/TiO_2 [70], polyamide6 (PA6)/Nylon6/TiO_2 [71], Ni-W-TiO_2 [72], SiO_2 on TiO_2-SiO_2 composite [73]. In addition, synthesizing nanomaterial based on their structure has been reported. The literature has suggested that the nanomaterials have been synthesized in various structures such as nanoflakes [74], nanoflowers [75,76], nanosheets [77], nanorods [78] and nanotubes [79].

2. Sensing processes of TiO_2

Depending on the desired application, the working principle for the various sensors is quite different. As shown in Fig. 4, TiO_2-based sensors can be classified into 3 common types based on the application: COD, gas, and bio-sensors. Though the applications are quite different, the sensing process is largely similar and can be summarized by the following steps (Fig. 5):

a) Binding between the receptor and analyte.
b) Signal production due to the chemical or biochemical reaction and reception by the transducer.
c) With an appropriate reference, the detector amplifies the previously converted electronic signals.
d) The signal is sent to computers for data processing and inspection of the results by the operator.

2.1. Measuring principle of biosensors

According to the sensing mechanism, the measuring principle of the biosensor can be classified into four major types: (a) potentiometry, and (b) amperometry.

Potentiometric methods: These methods are usually adopted in an electrochemical cell, where the potential signal is recorded from the accumulation of a charge potential when no significant current flows through the working electrode relative to the reference electrode. The literature is full of examples of the development of various field-effect transistor (FET) devices including light-addressable potentiometric sensors (LAPSs), ion-selective electrodes (ISEs), metal-oxide sensitive FETs (MOSFET), and ion-sensitive FET (ISFET). Amongst these types, ISFET and enzyme-modified ISFET devices are most widely used and investigated. The FET devices work on the principle of an electric field used to control the conductivity of a semiconductor film between two electrodes. The FET devices are widely used in the field of electrochemical biosensors as they can detect weak signals based on high impedance semiconductors.

Amperometry methods: Amperometric measurements are usually performed using a three-electrode system. A TiO_2 working electrode is combined with a counter and a reference electrode. These electrodes are connected to an electrochemical work-station which collects the current signals generated from the redox reactions of an electroactive species at a given potential. Based on the current collecting mode of the sensor, amperometry or voltammetry is used depending on the given potential dynamics. However, both give signals that are directly proportional to the bulk concentration of the analyte when measured over a linear potential range.

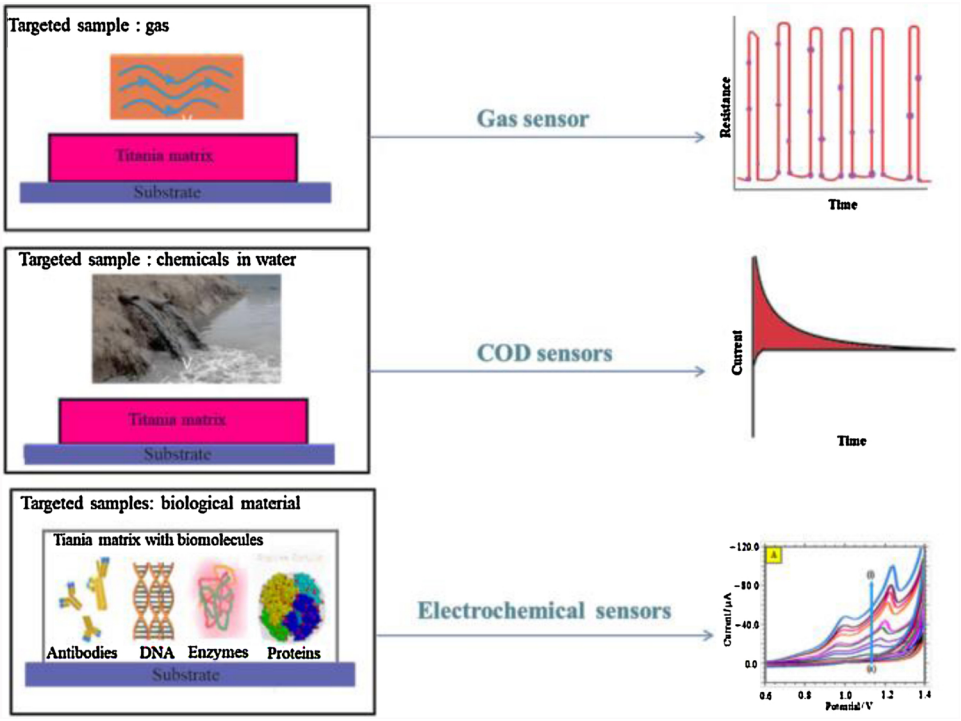

Fig. 4. TiO_2 based biosensors.

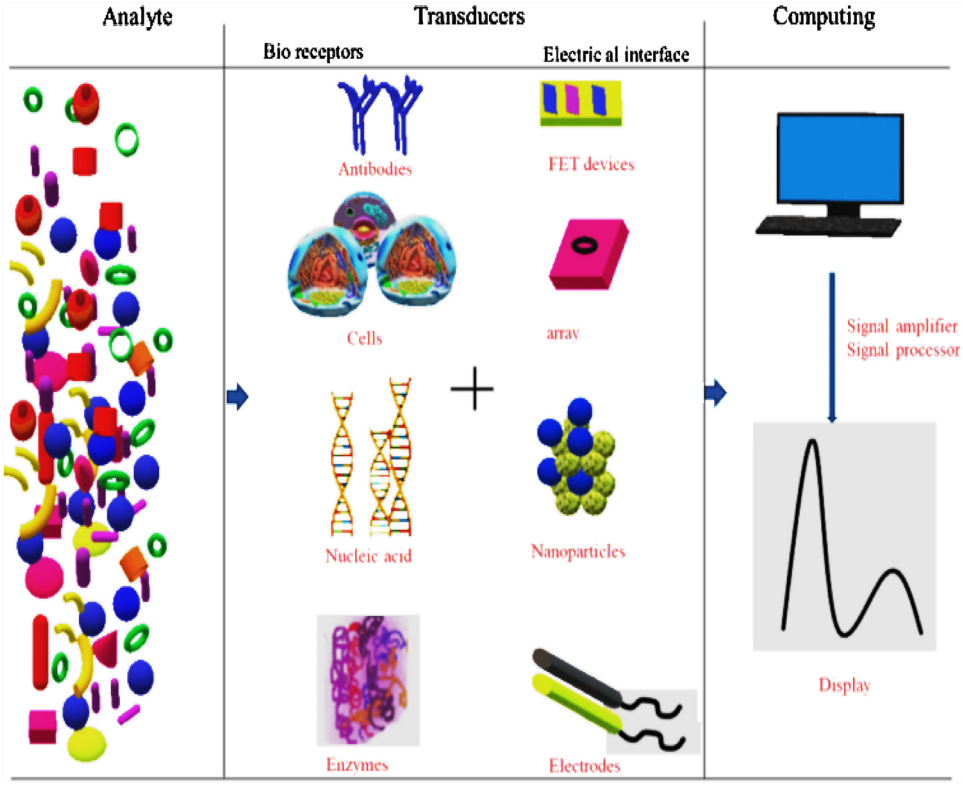

Fig. 5. Systematic presentation of biosensor working.

3. Electrochemical biosensors for medical applications

To advance point-of-care medical devices, electrochemical methods provide several advantages including simple design, miniaturization, low fabrication costs, low detection limits, and small operating volumes. The application of electrochemical biosensors in the medical field originated in 1962 with the study by Clark and Lyons regarding coupling between an oxygen electrode and glucose oxidase.

The authors created a simple and rapid blood glucose detector which was easily commercialized. Since then, many modern biosensors have been developed using various transducers and bio-recognition elements and have been extensively adopted for health monitoring. To develop bio-sensing devices with improved performance, TiO_2 nanomaterials, including nanoflowers [80], nanotubes [81], nanoparticles [82], composites [83,84], and nanosheets [85] coupled with antibodies, microorganisms, enzymes, and DNA have been fabricated.

3.1. Enzyme-based TiO_2 biosensors

To fabricate electrochemical enzyme biosensors, TiO_2 nanoparticles are excellent for immobilization and encapsulation of the relevant enzyme [83,84]. Recent studies have shown that long-term stability and enzyme bioactivity can be improved by using titania-modified electrodes. Various enzymes such as tyrosinase, urease, horseradish peroxidase (HRP), glucose oxidase (GOD), cytochrome c (cyt c), and glutamate dehydrogenase can be easily immobilized on the surface or inside of the TiO_2 nanostructure. The combination of multi-walled carbon nanotubes (MWCNTs) and TiO_2 nanoparticles represent a novel material for photoelectrochemical determination of lactic dehydrogenase. Characterization of the nanoparticle composite material suggested that the TiO_2 nanoparticles grown on the surface of the MWCNTs were anatase. The electrode regenerated nicotinamide adenine dinucleotide and was able to immobilize the enzyme on its surface. The hydrothermal method was used to grow the TiO_2 nanoparticles on the surface of the MWCNTs. The reports suggested that the regeneration of NAD+ holes was achieved by irradiating the MWCNT and TiO_2 composite. The MWCNTs present in the composite moved the electrons far away from the TiO_2 nanoparticles and prevented electron-hole recombination. The electrochemical experiments also suggested that the bioactivity of LDH and NAD+ was retained in the composite [86].

Liu et al. grew TiO_2 nanotubes on graphene nanoplatelets via the alkaline hydrothermal method [87]. Electrode modification was performed by simple application of the mixture of graphene, TiO_2, tyrosinase (Tyr), brominated 1-decyl-3-methylimidazole([Demim]Br), and Nafion on the glassy carbon electrode surface. The [Demim]Br is a room temperature ionic liquid used to improve the biocompatibility and electrical conductivity of the nanocomposite material. Nafion mediated graphene and tyrosinase immobilization on the electrode surface. The fabricated biosensor was used for the amperometric determination of catechol. Cyclic voltammograms recorded in presence (TiO_2|[Demim]Br|Nafion|Tyr|GCE) and absence (TiO_2|[Demim]Br|Nafion|GCE) of tyrosinase as an electrode modifier suggested that the reduction and oxidation peak currents for catechol on the TiO_2|[Demim]Br|Nafion|Tyr|GCE were increased by 68.5% and 39.3%, respectively. This was attributed to the catalytic effect of Tyr toward catechol redox. Furthermore, the voltammograms recorded in presence of graphene to form GNPs–TiO_2|[Demim]Br|Nafion|GCE in absence of Tyr and GNPs–TiO_2|[Demim]Br|Nafion|Tyr|GCE in presence of Tyr showed that the reduction peak increased by 215% and the oxidation peak of catechol disappeared. This was attributed to the exceptional flexibility and electrical conductivity of graphene that increased the electron transfer kinetics of the biosensor. Zhu et al. [88] fabricated an electrode using polyaniline (PANI) and TiO_2 nanotubes which provided low electrochemical interference, good electrical conductivity, and excellent biocompatibility. Glucose oxidase (GOD) was immobilized on the surface of the hydrothermally produced TiO_2 nanotubes on which aniline was polymerized. The immobilized GOD produced a voltammetric response due to electron exchange between the flavin adenine dinucleotide in GOD and electrode surface, as described by the following equation:

$$GOD\ (FAD) + 2e^- + 2H^+ \leftrightarrows GOD\ (FADH_2)$$

Tang et al. [89] loaded cholesterol oxidase on an electrode to improve the analytical performance of an electrochemiluminescent (ECL) biosensor for cholesterol on a nanocomposite comprised of Au nanoparticles/ion liquid/hollowed TiO_2 nano-shell on pre-functionalized ITO glass. As part of the nanocomposite catalysis, the enzymatically produced hydrogen peroxide intensified the ECL of luminol. The fabricated biosensor also showed the lowest detection limit compared to those of previously developed methods. This was attributed to the introduction of Au nanoparticles and hollow TiO_2 nanoparticles. The TiO_2 nanoparticles as a semiconductor generate e/h+ pairs which promote redox reaction of the molecule attached to the surface of the electrode. Furthermore, the reduced band gap due to the Au decoration results in the production of more e/h+ pairs. The small Michaelis–Menten constant confirmed the effective activity of cholesterol oxidase to catalyze the production of H_2O_2 via cholesterol oxidation.

An electrochemiluminescent biosensor based on Au/hollowed-TiO_2 nano-composite pre-functionalized electrode was proposed for the determination of cholesterol. Cholesterol oxidase was immobilized in presence of bovine serum albumin by cross-linking glutaraldehyde onto functionalized ITO [89]. For the diagnosis of diabetes, fast and reliable determination of blood glucose levels is important. The catalytic ability of glucose oxidase has been extensively used to fabricate electrochemical glucose biosensors. The development of third generation biosensors which use direct electron transfer (DET) between the electrode surface and FAD cofactor of the glucose oxidase without a mediator is the main goal of glucose detection. However, it is difficult to realize DET of the enzyme at the conventional electrode since the redox center in the biomolecule is located deep within the enzyme cavity.

Yang et al. [90] developed tetragonal columnar shaped TiO_2 (TCS-TiO_2) nanorods to immobilize glucose oxidase as part of a novel electrochemical glucose biosensor based on direct electrochemistry. The TCS-TiO_2 nanorods immobilized the enzyme to retain its bioactivity and structure with fast electron transfer through a surface-controlled and quasi-reversible process. Electron transfer between the electrode surface and enzyme was enhanced due to the large surface area of the TCS-TiO_2 nanorods. The voltammograms recorded using the modified GOx/TCS-TiO_2/chitosan/GCE showed distinct and well-defined peaks indicating that the TCS-TiO_2 improved the electrical contact between the electrode surface and redox active center of the enzyme, facilitating the direct electrochemistry of GOx. In addition, the larger surface area of the electrode increased the reduction peak current compared to that of other electrodes. In addition, the peak potentials for oxidation and reduction were separated by 54 mV, suggesting faster direct electron transfer between the electrode surface and redox-active site.

3.2. Doped TiO_2 nanoparticles

TiO_2 nanoparticles are photocatalytically active materials with reliable chemical properties, low toxicity, and low cost. However, the widespread application of TiO_2 nanoparticles is restricted in some fields due to its lower quantum efficiency due to easy recombination of photogenerated carriers and its wide band gap. To address these issues, methods such as non-metal and metal doping, as well as semiconductor coupling, have been used. TiO_2 nanoparticles doped with metals such as stanium, zinc, gold, and platinum have been used for photocatalysis, gas sensing, and humidity center. Due to its high chemical stability and superior photocatalytic activity, doped TiO_2 nanoparticles have also been used as biosensors. Doped TiO_2 nanoparticles have been used to increase optoelectrical performance, as doping can increase transparency and electrical conductivity as well as dramatically influence the sensing performance and crystalline structure of TiO_2 nanofilms.

Chou et al. [91] proposed a glucose biosensor composed of a ruthenium-doped TiO_2 sensing electrode fabricated using a co-sputtering system. A glucose biosensor was prepared by drop casting an enzyme composite onto the Ru/TiO_2 sensing film. Fabrication of the Ru/TiO_2 sensing film was achieved using a co-sputtering system consisting of a radio frequency power generator and DC power supply with titanium and ruthenium targets. Under a working pressure of 3×10^{-2} torr, the sensing film was deposited for 1 h at a growth rate of 7.9 nm/min. After annealing the Ru/TiO_2-based pH sensing film was packed using an epoxy resin. To immobilize the enzyme on the sensing film, a composite solution of glucose oxidase, 5 wt% Nafion, and 0.1 M phosphate buffer was dropped on the surface of the Ru/TiO_2 sensing film and then stored at 4 °C. The Ru/TiO_2 sensing film was observed to form a nanoflake-like structure. The sensing properties of the potentiometric glucose biosensor were analyzed in the concentration range of 100–500 mg/dL glucose using a voltage-time measurement system. Chen and Kafi [92] reported an amperometric biosensor based on Au-modified TiO_2 nanotube array-immobilized horseradish peroxidase and methylene blue with chitosan. The titania nanotube arrays were grown on a Ti substrate via anodic oxidation, and a gold thin film coating was deposited using the argon plasma technique.

The developed biosensor was used as a phenolic biosensor. The principle for the developed horseradish peroxidase modified electrode was the activation of HRP cycles by H_2O_2 to generate active oxyferryl radicals. By direct or indirect electron transfer to phenol, aromatic amines, ferrocenes, and amine ruthenium, the peroxidase immobilized on the electrode surface was reduced to its native state. Bukkitgar et al. [2] proposed an electrochemical method for the determination of atorvastatin. A composite electrode was prepared by fabrication of TiO_2 and clay nanoparticles. A technique such as cyclic voltammetry and square wave voltammetry was used for the investigations. The modified carbon paste electrode with TiO_2 nanoparticles and nano clay enhanced the response of atorvastatin about 4–5 times as compared to the bare carbon paste electrode. The proposed method had its application in the determination of atorvastatin in pharmaceutical dose form and human urine sample.

3.3. TiO_2-graphene hybrids-based biosensors

The extraordinary physical properties of graphene, including high specific surface area, chemical stability, and excellent charge carrier mobility, have garnered considerable attention. The two-dimensional layers of sp^2 bonded carbon and one atom thick structure of graphene is useful as supporting material for metal and metal oxide catalyst nanoparticles. Considerable attention has been recently paid to TiO_2-loaded graphene as an electrochemical biosensor. In addition to the superior properties such as high electrocatalytic activity and biocompatibility, TiO_2-graphene provides facile support for enzyme immobilization and direct electron transfer to enhance the electrochemical activity of the enzyme (Tables 1 and 2).

Liu et al. [93] prepared a titania nanoparticle modified reduced graphene oxide (TiO_2NPs-rGO) nanocomposite with immobilized hemoglobin as a mediator-free biosensor. The double-layered structure of the synthesized TiO_2NPs-rGO provided an excellent matrix for hemoglobin immobilization and facilitated direct electron transfer, improving H_2O_2 detection performance. Hemoglobin immobilization on the electrode surface with retention of bioactivity was achieved, as hemoglobin usually exhibits electrocatalytic activity toward H_2O_2, Cl_3CCOOH, and nitrite. The study used H_2O_2 as a probe to investigate the electrocatalytic activity of Nafion/Hb/TiO_2NPs-rGO/GCE (Nafion, hemoglobin TiO_2 nanoparticles reduced graphene oxide on glassy carbon electrode). The reaction was further studied using a titania nanosheet modified reduced graphene oxide (TiO_2NS-rGO) nanocomposite with immobilized hemoglobin to fabricate a mediator-free biosensor. Comparing the nanoparticles and nanosheets, improved sensor performance was observed in the linear range of 0.1–145 μM and the detection limit of the sensor was 10 nM.

Jang et al. [94] developed a glucose biosensor by adsorption of

Table 1
Type of hybrid TiO_2 nanostructures used for the biomedical application.

Nanomaterial type	Bio component	Technique used	LOD	Application in biochemical detection	Refs
Macro-mesoporous	HRP	Voltammetric	1.65 μM	H_2O_2	[108]
MoS_2-TiO_2@Au	DNA	Voltammetric	5×10^{-11} M	Tetracycline	[109]
Porous TiO_2	GOD	Amperometric		Glucose	[110]
TiO_2 nanotube array	GOD	Amperometric	5 μM	Glucose	[111]
Au/TiO_2 nanotubular	GOD	Voltammetric	–	Glucose	[112]
Pt/TiO_2 colloidal	GOD	Amperometric	0.25 μM	Glucose	[113]
(AuNPs)x/GR-TiO_2	HRP	Photoelectrochemical	0.02 pM	Thrombin	[114]
TiO_2 hollow nanofiber	GOD	Voltammetric	0.8 μM	Glucose	[82]
CP/MWCNT-Inulin-TiO_2	Urease	Voltammetric	0.9 μM	Urea	[115]

glucose oxidase on the surface of a TiO_2 graphene nanocomposite electrode. A colloidal mixture of TiO_2 nanoparticles and graphene oxide nanosheets were used to fabricate the TiO_2-graphene composite by aerosol assisted self-assembly (AASA). Morphological investigations of the synthesized composite revealed a spherical shape with graphene nanosheets encapsulating the micron-sized TiO_2 particles with a degree of encapsulation proportional to the ratio of graphene: TiO_2.

Boobphahom et al. [95] developed an electrochemical sensor based on nickel foam (Ni foam), titanium dioxide sol/graphene nanocomposite and lactate oxidase (LOx) successfully. 3D porous Ni foam electrode was coated with TiO_2/graphene nanocomposite to develop a novel electrode as an electrochemical biosensor. TiO_2 sol/graphene modified Ni foam offered a drastic increase in the current response as compared to unmodified Ni foam electrode for the detection of H_2O_2. Further, LOx was immobilized on the modified electrode for lactose sensor through H_2O_2 detection. The sensitivity and stability increased interestingly due to the combination between graphene and TiO_2 sol. In presence of ascorbic acid, dopamine, and glucose no interference was observed and a wide linear range of 50 μM–10 mM with a detection limit of 19 μM was reported for lactate.

3.4. Photoelectrochemical biosensors

Wang et al. [96] proposed a novel electrochemical biosensor for detection of microRNA-396a MoS_2/g-C_3N_4/black TiO_2 heterojunction as the photoactive material and gold nanoparticles carrying Histostar antibodies (Histostar@AuNPs) for signal amplification. Indium tin oxide electrode surface was deposited wihMoS_2/g-C_3N_4/black TiO_2 initially followed by gold nanoparticles and probe DNA was assembled on modified electrode surface. S9.6 antibody was used to recognize the hybridization with miRNA-396a which resulted in rigid DNA: RNA hybrid. The captured antibody can further conjugate with the secondary IgG antibodies of Histostar@AuNPs, thereby leading to the immobilization of horseradish peroxidase (HRP). The developed biosensor could detect miRNA-396a with a detection limit of 0.13 fM in the linear concentrations range from 0.5 fM to 5000 fM.

Cakiroglu et al. [97] proposed a light-sensitive hybrid material as a photoelectrochemical biosensor based on gold nanoparticles modified mesoporous TiO_2 coated on an indium tin oxide substrate, after a layer of MnO_2/g-C_3N_4. Further, β-galactosidase and Glucose oxidase were co-immobilized for glucose and lactose determination. The linear measurement ranges were calculated in the range of 0.004–1.75 mM, with a sensitivity of $1.54\ \mu A\ mM^{-1}\ cm^{-2}$ for glucose at 0 V, and 0.008–2.50 mM, with a sensitivity of $1.66\ \mu Am\ M^{-1}\ cm^{-2}$ for lactose at −0.4 V.

Wang et al. [98] fabricated CdS/$CuInS_2$/Au/TiO_2 nanotube arrays (NTAs) by deposition and dipping technique as well as successive ionic layer adsorption and reaction method. Improved interfacial electron transfer and quantum dots of CdS and $CuInS_2$ to form an ideal stepwise band edge structure with TiO_2 were obtained by using Au nanoparticles. By immobilizing HS-aptamer on the NTAs via Cd-S bond and Cu-S bond a photoelectrochemical aptasensor was fabricated for cytochrome c. The investigations were conducted successfully with a detection range of 5 pM–100 nM.

Qin et al. [99] designed a photoelectrochemical aptasensor based on graphene quantum dots-sensitized TiO_2 nanotube arrays (GQDs/TiO_2 NTs) for the detection of chloramphenicol. Coupling technique of linker molecule binding and electrophoretic deposition was used to prepare the nanohybrids. Through π–π stacking interaction between GQDs and the nucleobases of the chloramphenicol aptamer, immobilization of aptamers of chloramphenicol was demonstrated. A wide linear range from 0.5 nM to 100 nM for CAP detection with a low detection limit of 57.9 pM was reported.

3.5. Electrochemiluminescence biosensors

High sensitivity and selectivity of electrochemiluminescence (ECL) have proved ECL to be very useful in analytical applications. Its versatility, simplified optical setup compared with photoluminescence and temporal and spatial control compared to chemiluminescence ECL have presented outstanding advantages over other common analytical methods. The importance of ECL techniques for detection for bio-related applications have been well established and are heavily used in clinical lab applications commercially [100,101].

Zheng et al. [102] developed a ECL biosensor for sensing deoxynivalenol based on Luminol and tris(4,4′-dicarboxylicacid-2,2′-bipyridyl) ruthenium(II) dichloride ($Ru(dcbpy)_3^{2+}$) as a new ECL emitter units. In addition, surfactant assisted synthesized TiO_2mesocrystalsbeside serving as a matrix to accommodate Ru $(dcbpy)_3^{2+}$ it accelerated the electron transfer form reduced Ru $(dcbpy)_3^{2+}$ to oxidized $Ru(dcbpy)_3^{2+}$ facilitating ECL response of Ru $(dcbpy)_3^{2+}$. The process was established in a wide range from 0.05 pg/mL to 5 ng/mL with the detection limit of 1.67×10^{-2} pg/mL.

Fang et al. [103] proposed a ECL immunosensor for the analysis of deoxynivalenol based on bioprobe composed of TiO_2-B with fluoro-coumarin silicon phthalocyanine and luminol. The enhancement of ECL signal was owed to the large specific area favorable for increased loading of fluoro-coumarin silicon phthalocyanine which facilitated the decomposition of dissolved oxygen to generate reactive oxygen species participating in ECL reaction of luminol. The proposed immunosensor with high sensitivity and stability presented a advantageous performance in the linear range 1.0×10^{-6} ng/mL to 10 ng/mL with detection limit 3.3×10^{-7} ng/ml.

3.6. Amperometric biosensors

Amperometric sensing as compared to other sensing type utilizes only current measurements which can be obtained simply by two electrodes one to apply voltage and other to measure current.

Kadian et al. [104] successfully designed a method for glucose detection based on GOx which was immobilized on indium tin oxide/TiO_2/poly(3-hexylthiophene) nanohybrid film. The detection limit was observed to be of 0.620.02 mg/dL and 0.540.02 mg/dL in the standard buffer and human saliva samples, respectively. Further, the total time

Table 2
Electrochemical methods for the determination of an analyte using TiO_2 nanostructured hybrids.

Electrode material	Analyte	Linearity range	LOD	Refs
Graphene/TiO_2/V_2O_5	Chlorpromazine	3.30×10^{-8}–8.5×10^{-4} M	5.3×10^{-9} M	[115]
ZSM-5 nanozeolite-TiO_2 nanoparticles composite	Acetaminophen (AC), pramipexole (PRX) and carbamazepine	2.5–110, 0.6–105 and 6.0–97 μM	0.58, 0.38 and 1.04 μM	[116]
Ruthenium doped titanium dioxide nanoparticles	Clozapine	9.0×10^{-7} M to 4.0×10^{-5} M	0.43 nM	[117]
TiO_2 nanoparticles	Erythrosine.	0.1 μM–10.0 μM	2.6 nM	[118]
TiO_2-AuNPs- screen-printed carbon electrodes	Catechol	–	–	[119]
TiO_2-NT/WO_3	Endocrine disruptor propyl paraben	–	–	[120]
Molecularly imprinted film modified hierarchical branched titanium dioxide nanorods	Chlorpyrifos	0.01–100 ng/mL	7.4 pg mL^{-1}	[121]
Electrospun carbon nanofibers and TiO_2 nanoparticles	Idarubicin	0.012–10.0 μM	3 nM	[122]
CuO-TiO_2 hybrid nanocomposites	Methyl parathion.	0–2000 ppb	1.21 ppb	[123]
carbon paste electrode with a derivative of hydroquinone and TiO_2 nanoparticles	Phenylhydrazine (PhH) and hydrazine	2.0×10^{-6} to 1.0×10^{-3} M and 7.5×10^{-5}–1.0×10^{-3} M	7.5×10^{-7} M and 9.0×10^{-6} M	[124]
TiO_2 with a carbon paste electrode	Nicotine	2×10^{-6} M and 5.4×10^{-4} M	1.34×10^{-8} M	[125]
Nickel oxide nano flowers (3D-NiO) and TiO_2-nanowire arrays	Naringenin flavonoid	1.50×10^{-8} M to 2.35×10^{-4} M	0.025 nM	[126]
Titanium dioxide nanoparticles, multiwalled carbon nanotubes (MWCNT), chitosan and a novel synthesized Schiff base (SB) (TiO_2/MWCNT/CHIT/SB)	Thrombin	0.00005–10 nmol L^{-1}	1.0 fmol L^{-1}	[127]
Ruthenium-doped TiO_2 nanoparticles loaded into multi-walled carbon nanotubes	flufenamic acid	0.01–0.9 μM	0.68	[128]
Ruthenium-doped TiO_2 nanoparticles loaded into multi-walled carbon nanotubes	mefenamic acid	0.01–0.9 μM	0.45 nm	[128]
Silver-doped titania modified carbon electrode	Furantril	1.0×10^{-6} M to 1.2×10^{-8} M	1.98 nM	[129]
MWCNTs and Ru doped TiO_2 nanoparticles	Clozapine	0.01–0.07 μM	0.057 nM	[130]

taken for the detection of glucose saliva sample was less than 10 s suggesting a miniature device for detection of glucose for point-to-point care in medical application.

Paul et al. [105] proposed a new synthetic process using TiO_2 nanoparticles and glucose oxidase together encapsulated into the cavity of ZIF-8 metal–organic framework for establishing a glucose biosensor. Double layer capacitance and high surface area of TiO_2 increased catalytic activity of biosensor to detect low concentration level of 80 nM. The synthesized nanomaterial was drop-casted on glassy carbon electrode and Amperometry was used to obtain the sensor response.

3.7. Conductometric biosensors

Conductometric biosensors present a number of advantages such as thin film electrodes suitable for miniaturization and large scale production, no reference electrode, consumption of transducers are less, based on various reaction and mechanism large spectrum of compounds can be analyzed.

Maniruzzaman et al. [106] proposed conductometric biosensor for glucose based on GOx immobilized on TiO_2-cellulose hybrid nanocomposite. TiO_2-cellulose hybrid nanocomposite was prepared by blending TiO_2 nanoparticles with cellulose solution prepared by dissolving cotton pulp with lithium chloride/N,N-dimethylacetamide solvent. Further, the enzyme was immobilized by physical adsorption method. The linear response was reported in the range of 1–10 mM. Sadek et al. [107] proposed a nanoporousTiO_2 based conductometric sensors for detection of hydrogen (H_2) gas. The sensor responded with the highest sensitivity of 1.24 to 1% of H_2 gas at 225 °C.

4. Conclusion and future prospects

With unique properties such as large surface area, non-toxicity, environmentally friendliness, stability, and excellent biocompatibility, TiO_2 has performed exceptionally in physical, optical, chemical, photocatalytic, and electronic biosensors. These properties have also allowed TiO_2 nanomaterials to be applied for the detection of a variety of substances in COD, gas, and bio-sensors. The excellent biocompatibility of TiO_2 makes it an exceptional candidate for biosensor development. TiO_2-based biosensors have been incorporated into a variety of electrochemical/optical systems based on different sensing properties. Amperometric devices have provided the fastest and most accurate measurements to date. In recent years, research groups have focused on improving the performance of biosensors. The introduction of noble metals, as well as organic and inorganic compounds, may provide an alternative to develop novel nanomaterials with unique structures. The construction of smaller, cheaper, faster, and more efficient devices is a never-ending quest in the biosensor field, which may require seamless assimilation of biological and electronic systems.

Optimization of the properties and microstructure of TiO_2 materials is a popular research area. This popularity is driven by the need to develop effectual sensors with more advanced properties, improved accuracy, lower detection limits, and improved reproducibility. Detailed investigations of structure, morphology, electronic properties, and chemical composition should be performed in the future. In terms of healthcare applications, TiO_2 biosensors show great promise, but the popularity and adoption of these biosensors will depend on their reliability, awareness, cost, sophistication, availability, and marketing. Electrochemical sensors are simple, rapid, reliable, and inexpensive devices that can be used for clinical diagnoses with confidence. TiO_2 nanomaterials possess large surface areas as well as unique chemical, physical, optical, electronic, and photocatalytic properties, are non-toxic and environmentally friendly, and exhibit excellent biocompatibility and stability. These properties allow TiO_2 nanomaterials to be used to construct a wide range of sensing devices for biomedical applications. TiO_2 nanomaterials will be increasingly applied for the fabrication of electrochemical, photocatalytic, and

photoelectrocatalytic biosensors.

5. New trends in the development of TiO_2 hybride sensors for health care

Sensors are the heart of any measurement, control and diagnostics devices and termed as the critical component. In this review, we reported the usage of TiO_2 hybrid nanoparticles as a sensor for health care application. A recent glance of the literature has suggested that there are various methods for the synthesis of TiO_2nanohybrids. It is also clear that the recent investigation focused majorly on the application of these hybrids in health care. The use of electrochemical methods suggests that the proposed methods are time-saving, low cost, selective, sensitive and possibly be converted to miniature devices which very help in point-to-point care in medical application. Modification of electrodes with these nanohybrid structures has tremendously improved the analytical efficiency of electrochemical biosensors. These efforts have significantly lead to perform the investigations in wide linear range over pico/femto molar concentrations. These methods would further be an alternate platform for analysis replacing conventional analytical techniques.

Despite the significant progress achieved by nanohybrid TiO_2 in medical care synthesis of hybrid TiO_2 nanoparticles and modification of the electrode surface especially a specific antibody or aptamers requires a multistep process. Hence, future research has to focus on fabrication of electrode with simple and novel recombinant antibodies and aptamers offering sensors with rapid binding detection, high specificity under natural conditions and label-free. In addition, portable and disposable sensors with easy mechanism and methodologies are also need to be investigated. Further, serious chronic diseases such as cardiovascular, asthma, diabetes leading to large annual worldwide deaths have to be rectified. Finally, determined efforts in the development of these sensors for health care are still unavailable for end users and are restricted to laboratory scale.

References

[1] S.D. Bukkitgar, N.P. Shetti, R.M. Kulkarni, Sens. Actuators B Chem. 255 (2018) 1462.
[2] S.D. Bukkitgar, N.P. Shetti, Anal. Methods 9 (2018) 4387.
[3] A. Fujishima, K. Honda, Nature 37 (1972) 238.
[4] A. Fujishima, T.N. Rao, D.A.J. Tryk, Photochem. Photobiol. C 1 (2000) 1.
[5] D.A. Tryk, A. Fujishima, K. Honda, Electrochim. Acta 45 (2000) 2363.
[6] G. Sanzone, M. Zimbone, G. Cacciato, F. Ruffino, R. Carles, V. Privitera, M.G. Grimaldi, Superlattices Microstruct. 123 (2018) 394.
[7] K. Nemade, P. Dudhe, P. Tekade, Solid State Sci. 83 (2018) 99.
[8] A. Sahu, A. Dixit, J. Phys. Chem. Solids 122 (2018) 154.
[9] Z.O. Erdogan, I. Akin, S. Kucukkolbasi, Synth. Met. 246 (2018) 96.
[10] K.R. Reddy, K. Nakata, T. Ochiai, T. Murakami, D. Tryk, A. Fujishima, J. Nanosci. Nanotechnol. 11 (2011) 3692.
[11] W. Water, C.-W. Wen, J. Electroceram. 36 (2016) 94.
[12] Y. Lin, D. Li, J. Hu, G. Xiao, J. Wang, W. Li, X. Fu, J. Phys. Chem. C 116 (2012) 5764.
[13] G. Kaur, P. Negi, M. Kaur, R. Sharma, R.J. Konwar, A. Mahajan, Ceram. Int. 44 (2018) 18484.
[14] P. Ranka, V. Sethi, Al.Q. Contractor, Sens. Actuators B Chem. 261 (2018) 11.
[15] Z. Wei, X. Yang, Z. Mo, F. Leng, Sens. Actuators B Chem. 255 (2018) 3458.
[16] M.B. Askari, Z.T. Banizi, M. Seifi, S.B. Dehaghi, P. Veisi, Optik 149 (2017) 447.
[17] X. Wang, X. Xia, X. Zhang, W. Meng, C. Yuan, M. Guo, Mater. Sci. Eng. C 80 (2017) 174.
[18] C. Jia, T. Dong, M. Li, P. Wang, P. Yang, J. Alloy. Compd. 769 (2018) 521.
[19] M. Poloju, N. Jayababu, M.V.R. Reddy, Mater. Sci. Eng. B 227 (2018) 61.
[20] M. Bhattacharjee, D. Bandyopadhyay, Sens. Actuators A Phys. 285 (2019) 241–247.
[21] H. Shi, Y. Wang, J. Zhao, X. Huang, G. Zhao, J. Hazard. Mater. 342 (2018) 131.
[22] C.R. Zamarreño, M. Hernaez, P. Sanchez, I. Del Villar, I.R. Matias, F.J. Arregui, Proc. Eng. 25 (2011) 1385.
[23] Y.V.M. Reddy, B. Sravani, S. Agarwal, V.K. Gupta, G. Madhavi, J. Electroanal. Chem. 820 (2018) 168.
[24] E.M. Samsudin, S.B.A. Hamid, Appl. Surf. Sci. 391 (2017) 326.
[25] N.S. Peighambardoust, S.K. Asl, R. Mohammadpour, S.K. Asl, Electrochim. Acta 270 (2018) 245.
[26] K.R. Reddy, K.V. Karthik, S.B.B. Prasad, S. Soni, H.M. Jeong, A.V. Raghu, Polyhedron 120 (2016) 169.
[27] N.L. Reddy, V.N. Rao, M.M. Kumari, K.R. Reddy, P. Ravi, M. Shankar, Inamuddin, Environ. Chem. Lett. 16 (2018) 765–796.
[28] K.R. Reddy, K. Nakata, T. Ochiai, T. Murakami, D. Tryk, A. Fujishima, J. Nanosci. Nanotechnol. 10 (2010) 7951.
[29] S. Mathur, A. Erdemc, C. Cavelius, S. Barth, J. Altmayer, Sens. Actuators B 136 (2009) 432.
[30] J.R. Durrant, Anal. Chem. 70 (1998) 5111.
[31] Y. Kurokawa, T. Sano, H. Ohta, Y. Nakagawa, Biotechnol. Bioeneng. 42 (1993) 394.
[32] J.F. Kennedy, I.M. Kay, J. Chem. Soc. Perkin Trans. 1 (1976) 329.
[33] J. Tian, Y. Li, J. Dong, M. Huang, J. Lu, Biosens. Bioelectron. 110 (2018) 1.
[34] M.G. Miljković, V. Lazić, K. Banjanac, S.Z. Davidović, D.I. Bezbradica, A.D. Marinković, D. Sredojević, J.M. Nedeljković, S.I.D. Branković, Int. J. Biol. Macromol. 114 (2018) 1216.
[35] M.O. Silva-Moraes, Y. Garcia-Basabe, R.F.B. de Souza, A.J. Mota, R.R. Passos, D. Galante, H.D.F. Filho, Y. Romaguera-Barcelay, M.L.M. Rocco, W.R. Brito, Spectrochim. Acta Part A Mol. Biomol. Spectrosc. 199 (2018) 349.
[36] Y. Li, H. Cheng, N. Wang, Y. Zhou, T. Li, J. Alloy. Compd. 763 (2018) 421.
[37] A.K. Ayal, Z. Zainal, H.N. Lim, Z.A. Talib, Y.C. Lim, S.K. Chang, A.M. Holi, Mater. Res. Bull. 106 (2018) 257.
[38] K. Xie, Z. Wu, M. Wang, J. Yu, C. Gong, L. Sun, C. Lin, Electrochem. Commun. 63 (2016) 56.
[39] S. Mehraz, P. Kongsong, A. Taleb, N. Dokhane, L. Sikong, Sol. Energy Mater. Sol. Cells 189 (2019) 254.
[40] W. Ali, G.H. Jaffari, S. Khan, Y. Liu, Mater. Chem. Phys. 214 (2018) 48.
[41] W. Qi, J. Du, Y. Peng, W. Wu, Z. Zhang, X. Li, K. Li, K. Zhang, C. Gong, M. Luo, H. Peng, Mater. Chem. Phys. 207 (2018) 435.
[42] P.V. Viet, T.H. Huy, S.J. You, L.V. Hieu, C.M. Thi, Superlattices Microstruct. 123 (2018) 447.
[43] A. Azimi-Fouladi, S.A. Hassanzadeh-Tabrizi, A. Saffar-Teluri, Ceram. Int. 44 (2018) 4292.
[44] M. Yang, W. Liu, C. Jiang, S. He, Y. Xie, Z. Wang, Carbohydr. Polym. 197 (2018) 75.
[45] Y. Yan, V. Keller, N. Keller, Appl. Catal. B Environ. 234 (2018) 56.
[46] X. Wang, C. Zhang, L. Wang, T. Lin, G. Wen, Phys. B Condens. Matter 534 (2018) 39.
[47] X. Chen, X. Liu, X. Geng, Q. Jia, Ceram. Int. 44 (2018) 11204.
[48] J. Sung, M. Shin, P.R. Deshmukh, H.S. Hyun, Y. Sohn, W. Gyu Shin, J. Alloy. Compd. 767 (2018) 924.
[49] L. Barrientos, P. Allende, M.Á.L. Bercero, J. Pastrián, J.R. Becerra, L.C. Jensen, J. Phys. Chem. Solids 119 (2018) 147.
[50] H.R. Bakhsheshi-Rad, E. Hamzah, M. Daroonparvar, Safaa N. Saud, M.R. Abdulkadir, Vacuum 110 (2014) 127.
[51] B. Xiang, Y. Zhang, Z. Wang, X.H. Luo, Y.W. Zhu, H.Z. Zhang, D.P. Yu, J. Phys. D 38 (2005) 1152.
[52] A. Pearson, S.K. Bhargava, V. Bansal, Langmuir 27 (2011) 9245.
[53] J. Liu, W. Wang, T. Shen, Z. Zhao, H. Feng, F. Cui, RSC Adv. 4 (2014) 30624.
[54] A. Giampiccoloa, D.M. Tobaldib, S.G. Leonardic, B.J. Murdochd, M.P. Seabrab, M.P. Ansella, G. Neric, R.J. Ball, Appl. Catal. B Environ. 243 (2019) 183.
[55] T.E. Talane, P.S. Mbule, L.L. Noto, K. Shingange, G.H. Mhlongo, B.M. Mothudi, M.S. Dhlamini, Mater. Res. Bull. 108 (2018) 234.
[56] X. Wei, H. Cai, Q. Feng, Z. Liu, D. Maa, K. Chen, Y. Huang, Mater. Lett. 228 (2018) 379.
[57] N. Nithya, G. Bhoopathi, G. Magesh, C.D.N. Kumar, Mater. Sci. Semicond. Process. 83 (2018) 70.
[58] S. Mehraz, P. Konsong, A. Taleb, N. Dokhane, L. Sikongc, Sol. Energy Mater. Sol. Cells 189 (2019) 254.
[59] P.V. Viet, T.H. Huy, S.-J. You, L.V. Hieu, C.M. Thi, Superlattices Microstruct. 123 (2018) 447.
[60] Y.Y. Sun, Z.M. Zong, Z.K. Li, X.Y. Wei, Ceram. Int. 44 (2018) 3501.
[61] J. Ma, K. Wang, M. Zhan, ACS Appl. Mater. Interfaces 7 (2015) 16027.
[62] K.R. Reddy, H.M. Jeong, Y. Lee, A.V. Raghu, J. Polym. Sci. Part A Polym. Chem. 48 (2010) 1477.
[63] K.R. Reddy, B.Y. Sin, C.H. Yoo, D. Sohn, Y. Lee, J. Colloid Interface Sci. 340 (2009) 160.
[64] K.R. Reddy, W. Park, B.Y. Sin, J. Noh, Y. Lee, J. Colloid Interface Sci. 335 (2009) 34.
[65] K.R. Reddy, B.Y. Sin, J. Noh, Y. Lee, Synth. Met. 159 (2009) 1934.
[66] D.S. Rodríguez, M.G.M. Medrano, H. Remita, V.E. Barrios, J. Environ. Chem. Eng. 6 (2018) 1601.
[67] R.G.M. Oliveira, J.E.V. de Morais, G.S. Batista, M.A.S. Silva, J.C. Goes, A.S.B. Sombra, J. Alloy. Compd. 775 (2019) 889.
[68] Y. Zhu, Z. Cheng, W. Weng, K. Cheng, Colloids Surf. B Biointerfaces 172 (2018) 355.
[69] X. Hou, Y. Zhang, H. Ding, P.K. Chu, Particuology 40 (2018) 105.
[70] J.H. Yu, H. Yang, R.H. Jung, J.W. Lee, J.H. Boo, Thin Solid Films 664 (2018) 1.
[71] R. Singh, R. Kumar, I. Mascolo, M. Modano, Compos. Part B 143 (2018) 132.
[72] Y. Zhang, H.K. Bilan, E. Podlah, Electrochem. Commun. 96 (2018) 108.
[73] M. Zhang, E. Lei, R. Zhang, Z. Liu, Surf. Interfaces (2018), https://doi.org/10.1016/j.surfin.2018.10.005.
[74] G. Zu, H. Li, S. Liu, D. Li, J. Wang, J. Zhao, Sustain. Mater. Technol. 17 (2018) e00079.
[75] J. Ma, W. Ren, J. Zhao, H. Yang, J. Alloy. Compd. 692 (2018) 1004.
[76] K. He, Q. Wen, C. Wang, B. Wang, S. Yu, C. Hao, K. Chen, Chem. Eng. J. 349 (2018) 416.
[77] L.L. Qian, Y. Li, J.F. Li, C.W. Wang, Superlattices Microstruct. 117 (2018) 317.

[78] F. Zhan, W. Liu, H. Li, Y. Yang, M. Wang, Appl. Surf. Sci. 455 (2018) 476.
[79] J. Zhou, M. Guo, L. Wang, Y. Ding, Z. Zhang, Y. Tang, C. Liu, S. Luo, Chem. Eng. J. (2019), https://doi.org/10.1016/j.cej.2019.02.079.
[80] Y. Tang, P. Liu, J. Xu, L. Li, L. Yang, X. Liu, S. Liu, Y. Zhou, Sens. Actuators B Chem. 258 (2018) 906.
[81] J.A.V. Albelda, A. Uzunoglu, G.N.C. Santos, L.A. Stanciu, Biosens. Bioelectron. 89 (2017) 518.
[82] Q. Guo, L. Liu, M. Zhang, H. Hou, Y. Song, H. Wang, B. Zhong, L. Wang, Biosens. Bioelectron. 92 (2017) 654.
[83] B. Cakıroglu, M. Ozacar, Biosens. Bioelectron. 119 (2018) 34.
[84] P. Liu, X. Huo, Y. Tang, J. Xu, X. Liu, D.K.Y. Wong, Anal. Chim. Acta 984 (2017) 86.
[85] P. Pazhamalai, K. Krishnamoorthy, V.K. Mariappan, S.-J. Kim, J. Colloid Interface Sci. 536 (2019) 62.
[86] X. Liu, R. Yan, J. Zhu, X. Huo, X. Wang, Electrochim. Acta 173 (2015) 260.
[87] X. Liu, R. Yan, J. Zhu, J. Zhang, X. Liu, Sens. Actuators B 209 (2015) 328.
[88] J. Zhu, X. Liu, X. Wang, X. Huo, R. Yan, Sens. Actuators B 221 (2015) 450.
[89] S. Tang, Q. Zhao, Y. Tu, Sens. Actuators B 237 (2016) 416.
[90] Z. Yang, Y. Tang, J. Li, Y. Zhang, X. Hu, Biosens. Bioelectron. 54 (2014) 528.
[91] J.C. Chou, H.Y. Yang, C.W. Chen, Microelectron. Reliab. 50 (2010) 753.
[92] A.K.M. Kafi, A. Chen, Talanta 79 (2009) 97.
[93] H. Liu, C. Duan, X. Su, X. Dong, W. Shen, Z. Zhu, Ceram. Int. 40 (2014) 9867.
[94] H.D. Jang, S.K. Kim, H. Chang, K.M. Roh, J.W. Choi, J. Huang, Biosens. Bioelectron. 38 (2012) 184.
[95] S. Boobphahom, P. Rattanawaleedirojn, Y. Boonyongmaneerat, S. Rengpipat, O. Chailapakul, N. Rodthongkum, J. Electroanal. Chem. 833 (2019) 133.
[96] M. Wang, H. Yin, Y. Zhou, C. Sui, Y. Wang, X. Meng, G.I.N. Waterhouse, S. Ai, Biosens. Bioelectron. 128 (2019) 137.
[97] B. Çakıroğlu, Y.C. Demirci, E. Gökgöz, M. Özacar, Sens. Actuators B Chem. 282 (2019) 282.
[98] L. Wang, W. Gu, P. Sheng, Z. Zhang, B. Zhang, Q. Cai, Sens. Actuators B Chem. 281 (2019) 1088.
[99] X. Qin, Q. Wang, L. Geng, X. Shu, Y. Wang, Talanta 197 (2019) 28.
[100] W. Miao, Chem. Rev. 108 (2008) 2506.
[101] H. Wei, E. Wang, TrAC 27 (2008) 447.
[102] H. Zheng, Y. Ke, H. Yi, H. Dai, D. Fang, Y. Lin, Z. Hong, X. Li, Talanta 196 (2019) 600.
[103] D. Fang, X. Zheng, H. Yi, H. Dai, Z. Hong, Y. Peng, Y. Lin, Sens. Actuators B Chem. 283 (2019) 407.
[104] S. Kadian, B.D. Arya, S. Kumar, S.N. Sharma, R.P. Chauhan, A. Srivastava, P. Chandra, S.P. Singh, Electroanalysis 30 (2018) 1.
[105] A. Paul, D.N. Srivastava, ACS Omega 3 (2018) 14634.
[106] M. Maniruzzaman, S.-D. Jang, J. Kim, Mater. Sci. Eng. B 177 (2012) 844.
[107] A.Z. Sadek, J.G. Partridge, D.G. McCulloch, Y.X. Li, X.F. Yu, W. Wlodarski, K. Kalantar-zadeh, Thin Solid Films 518 (2009) 1294.
[108] X. Wu, H. Zhang, K. Huang, Y. Zeng, Z. Zhu, Bioelectrochemistry 120 (2018) 150.
[109] Y. Tang, P. Liu, J. Xu, L.L. Li, L. Yang, X. Liu, S. Liu, Y. Zhou, Sens. Actuators B Chem. 258 (2018) 906.
[110] S.J. Bao, C.M. Li, J.F. Zang, X.Q. Cui, Y. Qiao, J. Guo, Adv. Funct. Mater. 18 (2008) 591.
[111] P. Benvenuto, A.K.M. Kafi, A.C. Chen, J. Electroanal. Chem. 627 (2009) 76.
[112] M. Hosseini, M.M. Momeni, J. Solid State Electrochem. 14 (2010) 1109.
[113] D. Wen, S.J. Guo, J.F. Zhai, L. Deng, W. Ren, S.J. Dong, J. Phys. Chem. C 113 (2009) 13023.
[114] L. Wang, Y. Meng, Y. Zhang, C. Zhang, Q. Xie, S. Yao, Electrochim. Acta 249 (2017) 243.
[115] G.J. Kalaivani, S.K. Suja, Appl. Surf. Sci. 449 (2018) 266.
[116] S.K. Hassaninejad-Darzi, F. Shajie, Mater. Sci. Eng. C 91 (2018) 64.
[117] N.P. Shetti, D.S. Nayak, S.J. Malode, R.M. Kulkarni, Sens. Actuators B Chem. 247 (2017) 858.
[118] N.P. Shetti, D.S. Nayak, G.T. Kuchinad, J. Environ. Chem. Eng. 5 (2018) 2083.
[119] R. Gusmao, V.L. Puente, L. Yate, I.P. Santos, J.P. Juste, E.G. Romero, Mater. Today Commun. 11 (2017) 11.
[120] A.S. Martins, L. Nuñez, M.R. de VasconcelosLanza, J. Electroanal. Chem. 802 (2017) 33.
[121] X. Sun, C. Gao, L. Zhang, M. Yan, J. Yu, S. Ge, Sens. Actuators B Chem. 251 (2017) 1.
[122] E. Arkan, G. Paimard, K. Moradi, J. Electroanal. Chem. 801 (2017) 480.
[123] X. Tian, L. Liu, Y. Li, C. Yang, Z. Zhou, Y. Nie, Y. Wang, Sens. Actuators B Chem. 256 (2018) 135.
[124] F. Gholamian, M.A. Sheikh-Mohseni, H. Naeimi, Mater. Sci. Eng. C 32 (2012) 2344.
[125] M. Shehata, S.M. Azab, A.M. Fekry, M.A. Ameer, Biosens. Bioelectron. 79 (2016) 589.
[126] M.S. Prasad, R. Chen, H. Ni, K.K. Kumar, Arab. J. Chem. (2017) (corrected proof).
[127] E. Heydari-Bafrooei, M. Amini, M.H. Ardakani, Biosens. Bioelectron. 85 (2016) 828.
[128] N.P. Shetti, D.S. Nayak, S.J. Malode, R.R. Kakarla, S.S. Shukla, T.M. Aminabhavi, Anal. Chim. Acta 1051 (2019) 58.
[129] S.D. Bukkitgar, N.P. Shetti, R.M. Kulkarni, S.D. Kulkarni, ECS J. Solid State Sci. Technol. 7 (2018) Q3215.
[130] N.P. Shetti, D.S. Nayak, S.J. Malode, R.M. Kulkarni, ECS J. Solid State Sci. Technol. 7 (2018) Q3070.